Time-resolved biological and perturbation chemical crystallography: Laue and monochromatic developments

G. Bradbrook, A. Deacon, J. Habash, J.R. Helliwell*, M. Helliwell, Y.P. Nieh,

E.H. Snell, & S. Trapani

Department of Chemistry, University of Manchester
Manchester M13 9PL, U.K.

A.W. Thompson+ & J.W. Campbell

Daresbury Laboratory, Daresbury, Warrington, Cheshire, WA4 4AD, UK

N.M. Allinson & K. Moon

Department of Electronics, University of York, Heslington, York, YO1 5DD, UK

T. Ursby & M. Wulff

ESRF, BP220, Grenoble Cedex, France

*To whom correspondence should be addressed

+Present address: EMBL/ESRF, Avenue des Martyrs, Grenoble Cedex, France

ABSTRACT

Time-resolved macromolecular X-ray crystallography is a new capability for structural analysis driven by continuing improvements in synchrotron X-ray sources, optics and detectors (image plates and CCDs). Protein crystal Laue data (stationary crystal and polychromatic X-rays) were recorded at SRS Daresbury station 9.5 and ESRF Grenoble beamline 3, and processed with the Daresbury Laue software package. The Laue method allows exposure times set by the synchrotron electron bunch width, eg. 50 picoseconds. The instruments and methods developments widen opportunities for perturbation chemical crystallography studies too. A temperature dependent phase transition of a liquid crystal nickel-octahexylphthalocyanine is studied with a rapid readout CCD detector. Structure solution by molecular replacement methods with Laue data is reported for orthorhombic lysozyme. By use of tetragonal lysozyme as a test case it is shown that with fine angular intervals, wide total angular coverage of Laue exposures and the deconvolution of multiples, good connectivity of electron density maps can be realised. The monochromatic rotating crystal method offers possibilities of extremely fast rotations which allow a complete data set to be recorded onto a single image - Large-angle oscillation technique (LOT). The processed LOT data looks promising. LOT electron density maps are presented. We are now exploring the use of 360° rotations onto a single image. However, since the time required to cover one revolution of the crystal

0-8194-1880-3/95/$6.00

Downloaded From: http://opticalengineering.spiedigitallibrary.org/ on 02/17/2016 Terms of Use: http://spiedigitallibrary.org/ss/TermsOfUse.aspx

is likely to be greater than 1 millisecond, and because the monochromatic synchrotron radiation beam intensity sets its own limits to the shortest exposure time, the Laue method will retain its role for the fastest exposures in crystallography. Laue techniques open up quicker data collection opportunities in neutron protein crystallography.

Keywords: synchrotron radiation, CCD detector, liquid crystal transition, time-slicing, Laue method, LOT method, proteins, electron density, molecular replacement, lysozyme, neutrons. concanavalin A.

1 INTRODUCTION

Synchrotron radiation is now used extensively in macromolecular crystallography.[1] The first use of synchrotron radiation as a source for X-ray diffraction was directed at time-resolved biological fibre diffraction for the monitoring of the dynamics of muscle contraction.[2] Early considerations of the use of synchrotron radiation to measure data from crystalline samples included dynamical studies.[3] Data collection from protein crystals in general faces the major problems of weakness of reflections, a voluminous reciprocal space to be surveyed and radiation damage.[3] Time-resolved macromolecular crystallography[4] imposes yet further, major, demands since the quality of the determined protein structure must remain adequate whilst the single crystal data are measured rapidly and repeatedly, i.e. at specific time points.[5]

The fastest method of data collection uses a stationary crystal and a white X-ray beam (Laue method)[6]; it allows exposure times set by the synchrotron bunch width to measure a sizable region of diffraction (reciprocal) space but a full coverage is not realised in a single exposure. Hence a distinction is usefully made between X-ray exposure time and elapsed data collection time.[5] Better completeness is obtained, especially at low resolution, by monochromatic rotating crystal methods. By harnessing the collimation property of synchrotron radiation very large rotations can be covered in a single diffraction image; such a large-angle oscillation technique (LOT) allows the whole *lot* of data to be recorded onto a single image thus avoiding any time overheads of detector readout time.[7] The simultaneous translation of the detector and rotation of the crystal, over a more limited angular range, the Weissenberg method, as employed at synchrotron radiation sources[8] is also a monochromatic method advocated for fast data collection.[9] The Weissenberg method avoids overlapping of reflections but covers a restricted range of reciprocal space. LOT (section 4) offers a full coverage of reciprocal space but overlap of reflections is a problem at high resolution. The Laue method can achieve a high completeness at high resolution but the completeness at lower resolution is worse. A combination of Laue and LOT, with their complementary characteristics is therefore of interest. However, the Laue method has the pre-eminent role of allowing the fastest exposure times possible because all of the spectral emission from the synchrotron is condensed onto the crystal simultaneously in contrast to monochromatic rotating crystal methods where a tiny proportion of the synchrotron radiation emission is used (although this can be made more optimal by the use of an undulator to compress the white spectrum into specific, interference peaks in the emitted spectrum[1]). According to the type of structural change to be studied (reversible or irreversible) and its time constant the different tools, just referred to, of time-resolved simple crystal data collection can be applied. Time-resolutions of 50 picoseconds are accessible, at the ESRF 'Laue beamline' (BL3) where enough X-rays are focused onto a crystal to achieve a Laue photograph from one electron bunch circulating the ring.

The historical objection to the Laue method, that most of the Laue diffraction spots would be multiple (whereby Laue spots would comprise several reflections from interplanar spacings of d, $\frac{d}{2}$, $\frac{d}{3}$ etc. satisified by those wavelengths in the white spectrum λ, $\frac{\lambda}{2}$, $\frac{\lambda}{3}$ etc.)[6,10] has been analysed in detail[11]; the multiple orders problem is evidently not as serious as was initially believed since the proportion of reflections occurring alone in Laue spots never falls below 72.8%.[11] It is the remainder, however, that contribute to an under sampling of reflections at low resolution (large d spacing) as well as the shape of the volume of reciprocal space sampled by the Laue method. Improvements in detectors and computing, allow a much finer angular sampling of reciprocal space than hitherto. This will be dealt with in detail in section 3.4 (also section 2.2). The precise quantitation of Laue diffraction

Downloaded From: http://opticalengineering.spiedigitallibrary.org/ on 02/17/2016 Terms of Use: http://spiedigitallibrary.org/ss/TermsOfUse.aspx

intensity data has required the derivation and application of a wavelength-dependent correction (λ curve), to take into account a variety of source, instrument and sample induced variations in intensity at wavelengths in the broad bandpass. Strategies[12] have been put forward and methods[13] developed for singles and deconvolution of multiples in a Laue data set. These have been adequate to reveal a single water molecule in a protein of 30,000 molecular weight[14] and an accurate refinement of CO-myoglobin (including a partially occupied water molecule).[15] Further evidence that accurate Laue data and structural results are obtainable are provided in this paper (section 3).

2 INSTRUMENTATION

2.1 Low emittance sources and beamline designs for crystallography: Station 9.5 of the Daresbury SRS

Most of the analyses (Laue and LOT) presented here have been carried out with synchrotron data collected at station 9.5. This station design[16] takes advantage of the improvement of the emittance of the SRS (the so-called high brightness lattice) made in the mid 1980's whereby the point focusing function of the beamline optics is completely provided by the grazing incidence, doubly curved, mirror. Hence a point focused white beam ($0.5\mathring{A} < \lambda < 2.0\mathring{A}$) can be obtained of extremely high intensity opening up millisecond Laue crystallography (see fig.2 of ref.[17]). Moreover for monochromatic data collection rapid tunability is achieved via a double crystal, water cooled, channel cut monochromator and so multi-wavelength anomalous scattering data collection can be made[18] as well as high resolution data collection at short wavelengths (e.g. 0.7Å at SRS) much easier than on the other instruments at the SRS, 7.2[19] and 9.6.[20]

The station 9.5 beamline design concept lends itself to new, yet lower, emittance sources, like the ESRF (section 2.2), where the point focusing of the mirror allows the naturally small source size area to be even better matched to typical collimator(crystal) sizes ($\approx$0.2 mm). Very recent hardware improvements in the 9.5 hutch have been made consisting of a 3 axis goniometer[21] for protein crystal alignment which are certainly welcome allowing particular crystal sample settings in monochromatic[22] and Laue data collection[23] to be explored. The work reported in this paper (sections 3 and 4) is based, however, on a low cost, single axis, crystal orientation device.

In summary, the overall trend is for source emittance (source size $\times$ source divergence) to decrease. This has fitted the needs of protein crystallography extremely well as the sample acceptance (sample size $\times$ mosaicity) has thus become better matched by the source characteristics available.

2.2 Extremely fast exposure times in biological crystallography: The ESRF comes online (Beamline 3 and CCD detector)

The ESRF offers unprecedented brilliance, brightness and flux in the X-ray region for macromolecular crystallography,[24] extending up to high photon energies, compared with other current X-ray sources. Moreover the collimation can essentially reach a plane wave with a reasonable beam intensity at the sample. Combining such third generation synchrotron sources with detector developments such as the charge-coupled device (CCD) has and will continue to result in improved detector time response and quality of data available.

We have conducted experiments on BL3[25] of the ESRF with a CCD[26] detector probing the data quality that can be obtained. For example, nine Laue images from tetragonal lysozyme were collected at 1° intervals, 20 millisecond exposure time, for calibration and spatial uniformity response checks. The data were processed using the Daresbury Laue suite[13] to 2Å resolution in the wavelength range 0.28 to 2.5Å. For wavelength normalisation a

Downloaded From: http://opticalengineering.spiedigitallibrary.org/ on 02/17/2016 Terms of Use: http://spiedigitallibrary.org/ss/TermsOfUse.aspx

range of 0.43 to 0.90Å was used. The normalisation curve is shown in figure 1a, the peak at 0.55Å is at a very much shorter wavelength than data collected at previous synchrotron sources such as the SRS wiggler.[13] The R_{merge} is 8.8% on I. By comparing the wavelength-normalised data from one image with a reference monochromatic

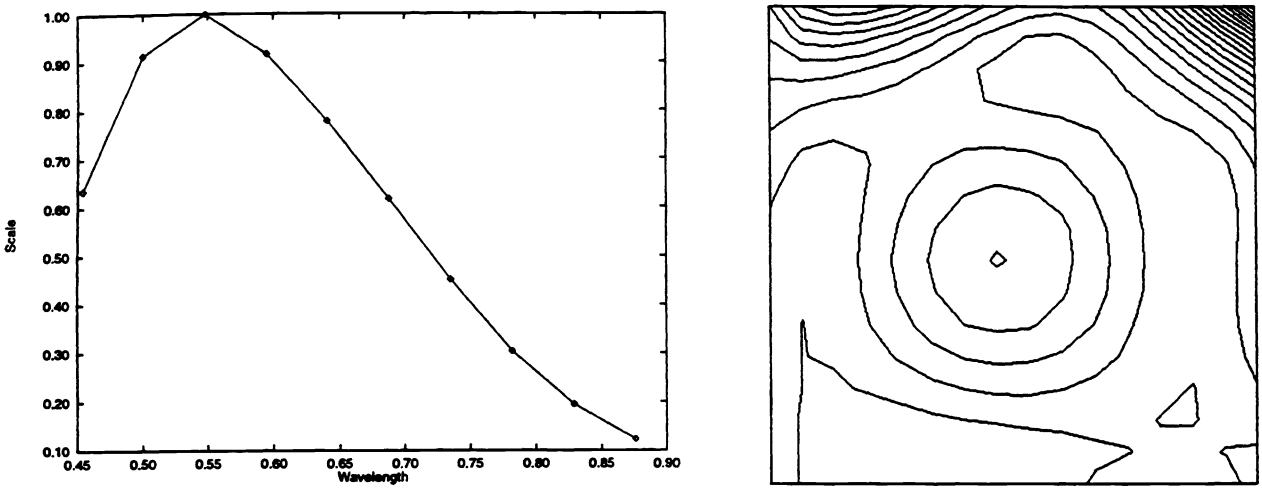

(a) (b)

Figure 1: ESRF BL3 with CCD Laue data from a tetragonal lysozyme test crystal (a) Wavelength normalisation curve, wavelength is given in Å. (b) Contour plot of the spatial response derived from LAUESCALE of the CCD detector; contours are in 5% response levels down from 100% at the centre of the detector.

(diffractometer) data set using the Daresbury program LAUESCALE it is possible to calculate the detector non-uniformity of response. One such contour plot is shown, figure 1b, which is applied to the raw image and the data reprocessed (a sort of post-refinement technique).

2.3 Rapid readout CCD detectors and perturbation chemical crystallography: Space group transition of nickel-octahexylphthalocyanine as a function of temperature

There exists considerable promise for the use of CCD imagers in the fast recording of diffraction patterns. These devices complement the use of micro-spectrophotometric monitoring of reactions in crystals where a chromophore is present but uniquely give insight into the crystal diffraction quality. When a chromophore is not present such time-slicing could be the only guide to crystal structure monitoring as a function of time. As part of the development of such devices we have described the first tests of very short (80 millisecond) protein crystal Laue diffraction exposures.[27] Subsequently tests of intensity reproducibility showed merging R-factors on I of 3%.[28] A time-resolved study of radiation damage to a protein crystal was then made involving the repeated measurement of a part of the Laue pattern over a period of 4.2 seconds and showed the steady increase in crystal mosaic spread with exposure.[5] These developments offer application too in perturbation chemical crystallography. A review of this topic can be found in ref.[29]

Here we report the use of a CCD detector[30] to determine the transition temperature from one crystal space group to another, of nickel octahexylphthalocyanine. This becomes a thermotropic liquid crystal at 140°C. Between room temperature and liquid nitrogen temperature the crystal undergoes another transition. By starting at 100K and raising the temperature stepwise, the CCD diffraction pattern was recorded at each temperature on station 7.2 of the SRS[19] with a monochromatic beam. The CCD was coupled to a 2.6:1 fibre optic taper with a structured CsI(Tl) scintillator grown directly onto the front. The image consists of 576 × 384 pixels with each pixel being 58.5 μm square giving a total aperture of 33.7 × 22.5 mm. The system is optimised for fast readout,

Downloaded From: http://opticalengineering.spiedigitallibrary.org/ on 02/17/2016 Terms of Use: http://spiedigitallibrary.org/ss/TermsOfUse.aspx

≈100 milliseconds at 12 bit dynamic range. A disadvantage of the test made with the monochromatic beam was the rather long exposure times required which led to a noise build up. This would not be a problem in general with a polychromatic beam, or a stronger monochromatic beam. Nevertheless the experiment performed allowed the determination of the transition temperature within only a few hours of beamtime. A disappearance of spots due to $h + k = 2n + 1$ occurred between 195 to 200K representing the change between the low temperature primitive crystal lattice and the higher temperature C-centred crystal lattice (figure 2). The structural details of this transition will be described elsewhere.

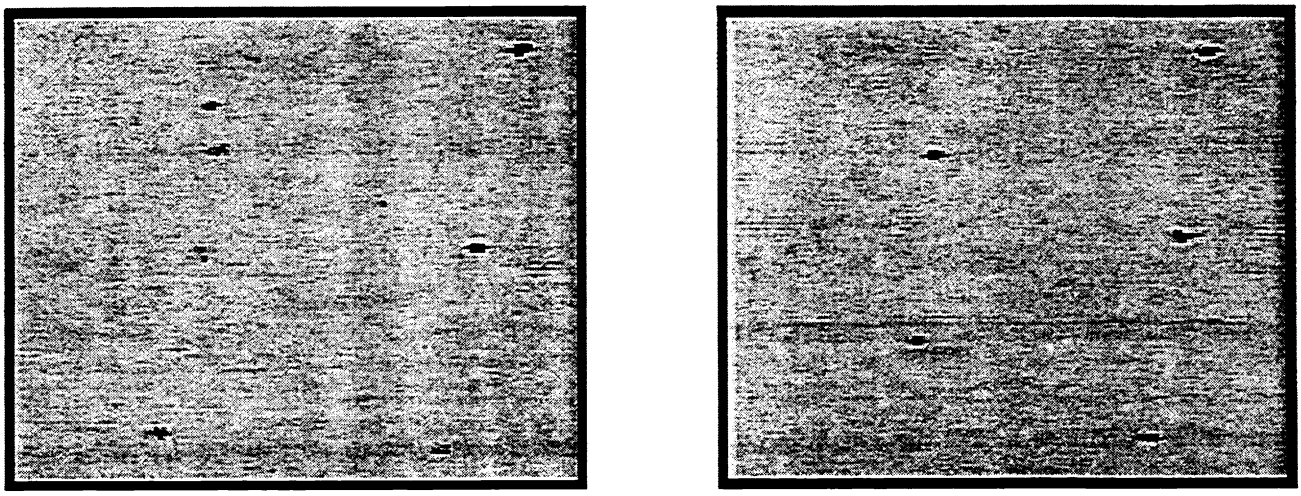

Figure 2: Two of the CCD images showing a disappearance of spots due to $h + k = 2n + 1$ occurring between 195K (left) to 200K (right) representing the change between the low temperature primitive crystal lattice and the higher temperature C-centred crystal lattice

3 LAUE PROTEIN CRYSTAL STRUCTURE ANALYSES: NEW DEVELOPMENTS AND RECENT CHALLENGES

Recent challenges to the Laue method for structural studies of proteins have included the impact of the distribution of those reflections tied up in 'multiple' Laue spots,[11] particularly with respect to fragmentation (connectivity) of certain electron density maps (e.g. 2Fo-Fc), and also identifying atoms with high B-factors in a structure.[31] Moreover, our wavelength normalisation[13] has been criticised[32] in terms of the uncertainty of the scale factors, in spite of the concordance of scale factors shown in our ('Daresbury' package) broad wavelength band protein crystal Laue data and processing[13] and the structural results obtained.[14,15]

Of considerable interest to us have been the new experimental opportunities for Laue data collection afforded by automatic readout detectors, and of enhanced sensitivity, such as on-line image plates and CCDs. The enhanced sensitivity allows fairly small protein crystals to be used for Laue data collection (section 3.2). These detectors also circumvent the labour of Laue *photography*. Hence a much finer angular interval between Laue exposures can be obtained within the required coverage of a given crystal symmetry. This will allow a much better completeness at low resolution to be more readily achieved (examples at different angular intervals are given in section 3.4 below).

Downloaded From: http://opticalengineering.spiedigitallibrary.org/ on 02/17/2016 Terms of Use: http://spiedigitallibrary.org/ss/TermsOfUse.aspx

3.1 Obtaining higher resolution Laue data: 2.0Å versus 2.5Å tetragonal lysozyme

Obtaining high resolution Laue data with a broad bandpass beam is practical as evidenced in our previous study of carbonic anhydrase[14] (2.2Å high quality data). Likewise, for native concanavalin A, broad bandpass Laue data yielded a resolution limit of 2.4 Å, but restricting the bandpass (using an Al filter) however, reduced the background allowing a prolonged exposure time yielding data to 1.95Å.[7] An automatic control of λ_{max} is clearly important for bandpass limitation and for this reason we have developed a transmission mirror based on thin mylar films.[33,34] We now report on similar results for chicken egg white lysozyme. By restricting the bandpass (0.2 mm Al filter) and using longer exposure times (750 millisececonds versus 250 milliseconds), for similar machine ring currents, the resolution limit is enhanced from 2.5Å to 2.0Å.

A tetragonal lysozyme crystal (a=b=79.1Å, c=37.9Å, $P4_32_12$) was used to collect Laue data on station 9.5[16] of the SRS. The SRS operated at 2.0 GeV and 196 mA with the wiggler at 5T. The collimator diameter of 0.2 mm was smaller than the crystal in each dimension. Data were collected on an image plate detector (MAR research) of 90 mm radius placed 204 mm from the crystal. Five images were collected in 12° degree intervals covering 0-48°. Laue images were processed using the Daresbury Laue suite of programs[13] to obtain singles data, deconvoluted multiples data and finally a combined set of singles and deconvoluted multiples. Deconvolution used the wavelength normalisation curve method.[35] At the normalisation stage reflections stimulated within the wavelength range 0.52-1.60Å were used. The combined singles and deconvoluted multiples data set contained 6342 reflections with completeness $d_{min} - \infty$ of 74.1%, $d_{min} - 2d_{min}$ of 77.9% and $2d_{min} - \infty$ of 50.5% with an R_{merge} of 8.8%. For comparison the singles data had a completeness $d_{min} - \infty$ of 67.7%, $d_{min} - 2d_{min}$ of 72.5% and $2d_{min} - \infty$ of 37.4%.

The original Protein Data Bank (PDB filename 6LYZ) coordinates[36] were refined with the X-PLOR program.[37] Each cycle of refinement included 40 cycles of positional refinement followed by 20 cycles of temperature factor refinement. Map calculations were carried out with the CCP4 program suite[38] and maps were inspected with the program FRODO[39] and later O.[40] Refinement converged with an R-factor of 21.0%, geometric rms deviations of 0.011Å for bond lengths, 2.0° for bond angles and 22.6° for torsion angles. The average temperature factors for the main and side chain atoms were 13.3Å^2 and 17.7Å^2 respectively. There were 80 water molecules with an average temperature factor of 25Å^2. Inspection of the Ramachandran plot[41] showed 100% of all non-glycine and non-proline residues lying in the most favoured and additional allowed regions. For comparison the singlet Laue data set yielded a final R-factor of 19.3% in model refinement for 5792 reflections with 63 common water molecules in good density and chemically sensible positions.

The study showed in general that the combined data set gave improved electron density connectivity for the main and side chains. For TRP, PHE, TYR, HIS and PRO residues, the combined data set gave pronounced improvements in the electron density but did not enhance the number of water molecules (80 versus 77). The benefits in reaching higher resolution are evident in the increase in the number of reflections over earlier studies[42] at 2.5Å (2573 single, 2963 combined) for refinement of the model.

3.2 Small protein crystals: Synchrotron Laue study of orthorhombic lysozyme including molecular replacement

Orthorhombic chicken egg white lysozyme crystals (obtained unexpectedly from the crystallization conditions for tetragonal lysozyme[43]) have been studied using synchrotron Laue diffraction. Laue data to 3Å were collected on station 9.5 of the SRS[16] on a relatively small crystal ($\approx 0.08 \times 0.10 \times 0.50$ mm) using an image plate (MAR research). The SRS was operating at 2.0 GeV and 262 mA, a 0.2 mm thick Al foil was used to attenuate the long wavelength (radiation damaging) parts of the beam giving a band pass of $0.4 < \lambda < 2.0$Å. The collimator diameter was 0.2 mm. A total of 15 exposures were recorded over a range of 140° in 10° intervals with a 400 millisecond exposure time per image. Unit cell dimensions for $P2_12_12_1$ orthorhombic lysozyme[44] (a=59.4Å,

Downloaded From: http://opticalengineering.spiedigitallibrary.org/ on 02/17/2016 Terms of Use: http://spiedigitallibrary.org/ss/TermsOfUse.aspx

b=68.7Å, c=30.8Å) were used in the determination of crystal orientation with LAUEGEN.[45] An example of one image obtained is shown in figure 3a. The data were processed using the Daresbury Laue software suite[13] and reduced using the CCP4 suite of programs[38] giving an overall R-factor on I of 7.2%, 1843 unique reflections and average multiplicity of 5.8. The completeness ranges are $d_{min} - \infty$ of 88.4%, and $2d_{min} - \infty$ of 37.3%.

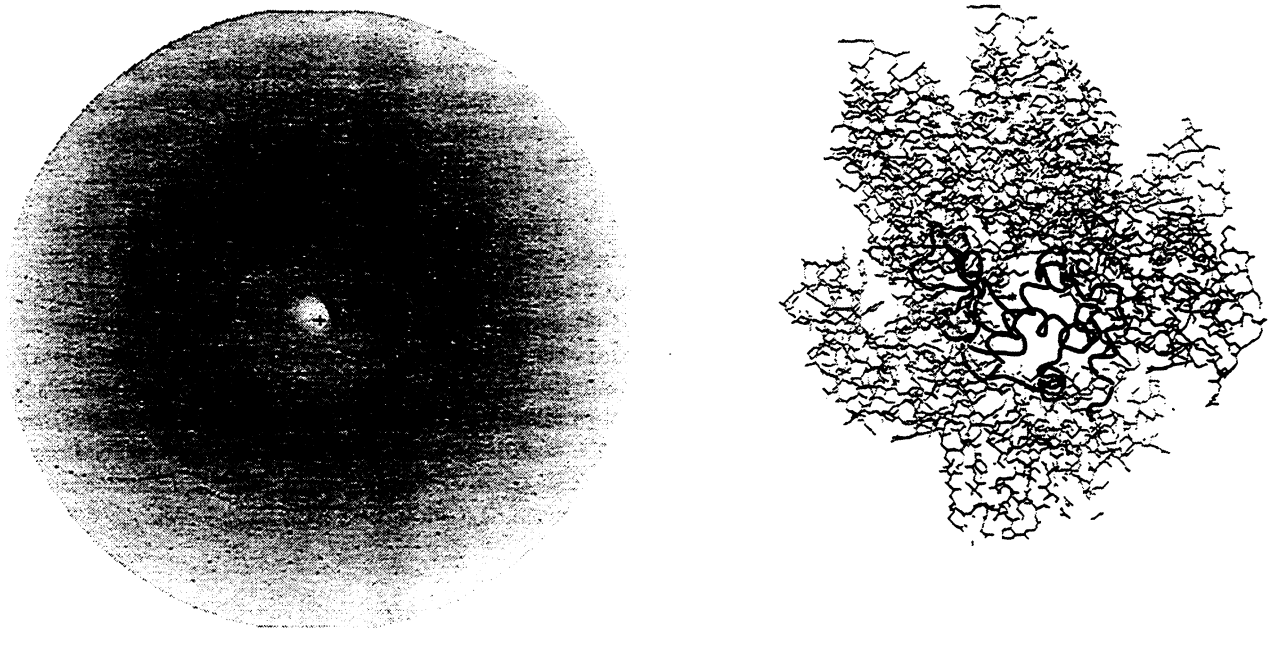

(a) (b)

Figure 3: (a) Laue diffraction pattern from a small crystal of orthorhombic lysozyme (b) The resulting structure showing the accessibility of saccharide binding sites D, E and F (indicated by * in the centre) via the solvent channels for orthorhombic lysozyme.

These data were used to provide an initial molecular model using the MERLOT molecular replacement package.[46] The starting model was that of 2.0Å resolution tetragonal lysozyme deposited at the PDB (6LYZ).[36] The rotation and translation results obtained were as follows:

Euler rotation angles(°)	108.00	67.00	34.00
Translation (as a fraction of unit cell edge)	0.466	0.367	0.007

After rigid body refinement of the molecular replacement solution the R-factor on F was 40% indicating that an essentially correct solution had been found. Graphics images of this crystal form of the enzyme clearly show that the saccharide binding sites D, E and F are accessible via solvent channels (figure 3b), which is in agreement with the earlier, MIR monochromatic results to 6Å.[44]

Data have also been collected to a higher resolution (2Å) at the NSLS and ESRF on sugar soaked crystals with a view to undertaking the detailed refinement of the protein in this crystal form and hopefully complexed with sugar. On a technical note it is impressive that crystals of this size could be used and is testimony to the improved sensitivity of modern detectors (such as image plates and CCDs) over photographic film.

Downloaded From: http://opticalengineering.spiedigitallibrary.org/ on 02/17/2016 Terms of Use: http://spiedigitallibrary.org/ss/TermsOfUse.aspx

3.3 Improved Laue software procedures: Reprocessing and re-refinement of cobalt concanavalin A using Laue image plate data

Using an improved version of the Daresbury Laue software suite including LAUEGEN[45] we have repeated a previous study[33] on Co concanavalin A. A larger number of reflections has then been made available.

Laue data from a single crystal of Co concanavalin A (a=88.7Å, b=86.5Å, c=62.5Å, I222) were collected[33] on station 9.5 of the SRS[16] using a relatively narrow bandpass ($0.5\mathring{A} < \lambda < 0.9\mathring{A}$) to a resolution of 2.0Å. A total of fifteen images were collected covering an angular range of 122° and processed with the Daresbury Laue suite of programs.[13]

The singles data were reduced using the CCP4[38] suite of programs giving completeness of $d_{min} - \infty$, 80.8%, $d_{min} - 2d_{min}$ of 84.1% and $2d_{min} - \infty$ of 59.0% with an R-factor on I of 7.9%. The previous study gave a completeness of $d_{min} - \infty$, 76.5%, $d_{min} - 2d_{min}$ of 80.5% and $2d_{min} - \infty$ of 51.6% with an R-factor on I of 7.7%. In terms of the number of independent reflections, with the improved software we obtained 13436 unique reflections compared with the 12723 reflections from the previous study.

A starting set of coordinates from a monochromatic 2Å study of a Cd substituted concanavalin A, also in space group I222[47] has been used for the structure refinement.

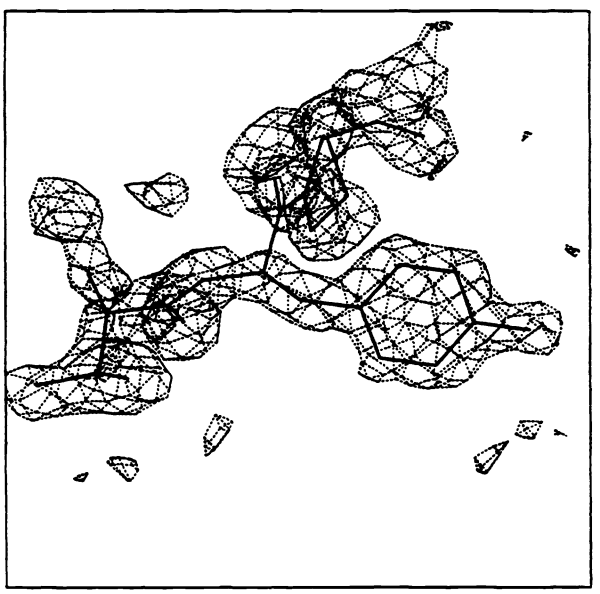

Figure 4: 2Fo-Fc map at 1.5σ level showing the Tyr 12 residue from Co concanavalin A

The water molecules were deleted from the starting coordinate set, the positional and B-factor refinement has been carried out using X-PLOR,[37] followed by difference Fourier map calculation[38] and model building using O.[40] The procedure has been repeated until convergence. During the model building residues 151 and 155 have been changed from Glu to Asp and Arg to Glu respectively. The side chain conformations of Ser 21, Asn 41, Asp 136, Ser 160, Glu 183 and the main chain conformation of Thr 150 have been changed to get the best fit of the model to the electron density map. A total of 126 waters have been added to the model. At convergence the R-factor was 18.2%, geometric rms deviations of 0.007Å for bond lengths and 1.931° for bond angles. Figure 4 shows the Tyr 12 residue.

The goodness of the geometry of the model has been checked using PROCHECK.[48] No residues were in unfavourable regions. The 2Fo-Fc map contoured at the 1σ level shows generally good connectivity along the main chain, apart from the loop regions of the protein (especially in the region of residues 116 to 124 where the map is very poor).

3.4 Filling the low resolution hole in Laue data using fine angular interval data collection for tetragonal lysozyme

Good quality lysozyme crystals were available to us from experiments that were conducted aboard the Spacehab-1 NASA Space Shuttle mission.[49,50] Utilising these crystals and ground controls Laue data were col-

Downloaded From: http://opticalengineering.spiedigitallibrary.org/ on 02/17/2016 Terms of Use: http://spiedigitallibrary.org/ss/TermsOfUse.aspx

lected on station 9.5 of the Daresbury Synchrotron Radiation Source.[16] A MAR image plate detector was used to record 31 images at 2° intervals each with an exposure time of 500 ms from one of the microgravity grown crystals. A ground control crystal was used to collect 23 images at 3° intervals again with 500 ms exposure time. The synchrotron was operating at 2.0 GeV with an average current of 210 mA during the data collection run. To attenuate the longer wavelengths a 0.4 mm aluminium foil was used in the beam path.

The data were processed using the Daresbury Laue processing suite[13] with a λ_{min} of 0.40Å, λ_{max} of 1.55Å and d_{min} of 2.50Å. Data reduction used the CCP4 programs[38] ROTAVATA and AGROVATA.

To study the effects of data collection at different angular intervals several subsets of the data were examined; the complete data set of 31 images from the microgravity crystal making up 60° in 2° intervals, 16 images making up 60° in 4° intervals, 6 images making up 60° in 10° intervals and finally 3 images with 30° degree intervals. The data were processed using firstly singlets only and secondly with multiplet deconvolution[35] and the resulting completeness of both data sets is shown in figure 5. The low resolution cutoffs at 50% completeness are shown providing evidence of the complementary nature of LOT (section 4) to Laue data collection.

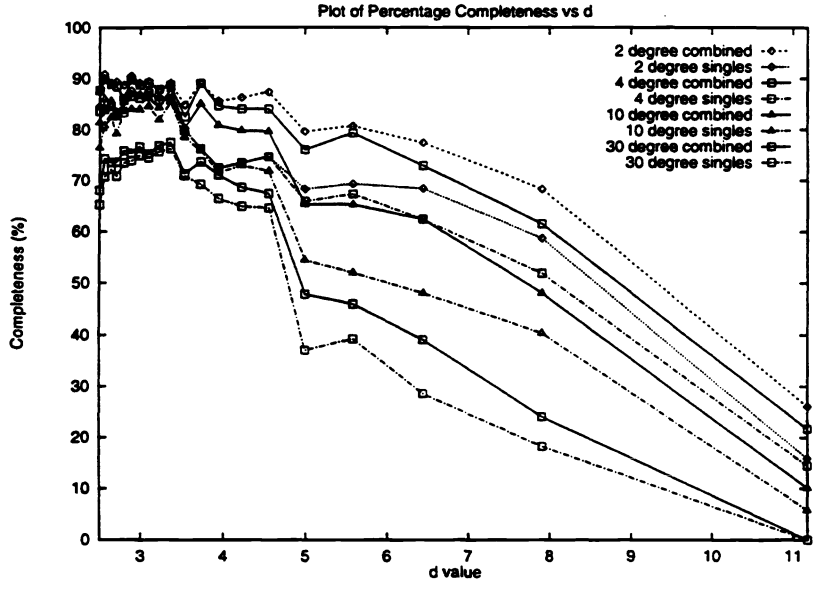

$\Delta\phi$	singles d_{max} Å	combined d_{max} Å
2°	8.6	9.3
4°	8.1	8.9
10°	6.0	7.8
30°	4.9	5.0

Figure 5: Percentage completeness vs d values for Laue data from tetragonal lysozyme crystals collected at station 9.5. Data are shown at 2, 4, 10, and 30° angular intervals respectively for an overall angular range of 60°. Low resolution cutoffs at 50% completeness for protein crystal Laue data have been extracted from the graph to illustrate the interest in low resolution LOT data between $d_{max} < \lambda < \infty$ Å.

The data were used to refine the structure of lysozyme against coordinates deposited at the PDB, (6LYZ),[36,51] as a starting model using the program XPLOR.[37] Subsequently electron density maps were calculated using the CCP4[38] software package and the model fitted to the maps manually using FRODO[39] and later O.[40]

The effect of the improved completeness at low resolution using the combination of small angular steps and multiplicity deconvolution is manifest in the electron density maps. Figure 6 shows this clearly by homing in on the Phe 38 residue. The connectivity of the map at the 2° angular resolution step is good but quality decreases, as would be expected, towards larger angular intervals in a gradual way. The real space R-factors (RSR) are plotted per residue for each Laue data set in figure 7. Hence the ease with which recently available automatic readout detectors can be utilised is important, as is the extra sensitivity of those devices over photographic film in realising routine measurement of many more Laue diffraction images per crystal.

Downloaded From: http://opticalengineering.spiedigitallibrary.org/ on 02/17/2016 Terms of Use: http://spiedigitallibrary.org/ss/TermsOfUse.aspx

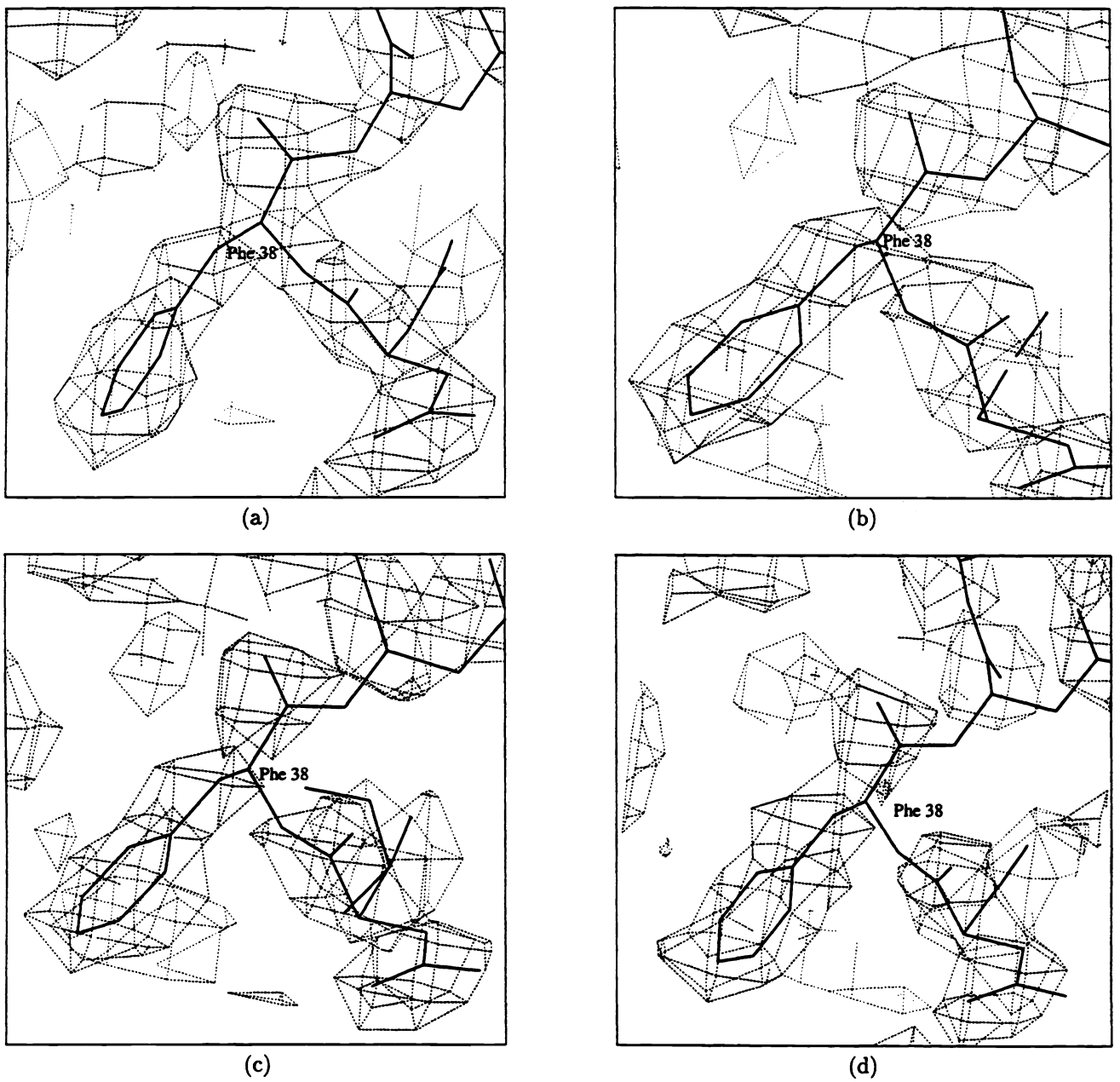

Figure 6: 2Fo-Fc Laue electron density maps at the 1σ level showing the Phe 38 residue in tetragonal lysozyme for data collected with (a) 2° angular steps, (b) 4° angular steps, (c) 10° angular steps, and (d) 30° angular steps. Total angular coverage of 60°. For details see section 3.4.

Downloaded From: http://opticalengineering.spiedigitallibrary.org/ on 02/17/2016 Terms of Use: http://spiedigitallibrary.org/ss/TermsOfUse.aspx

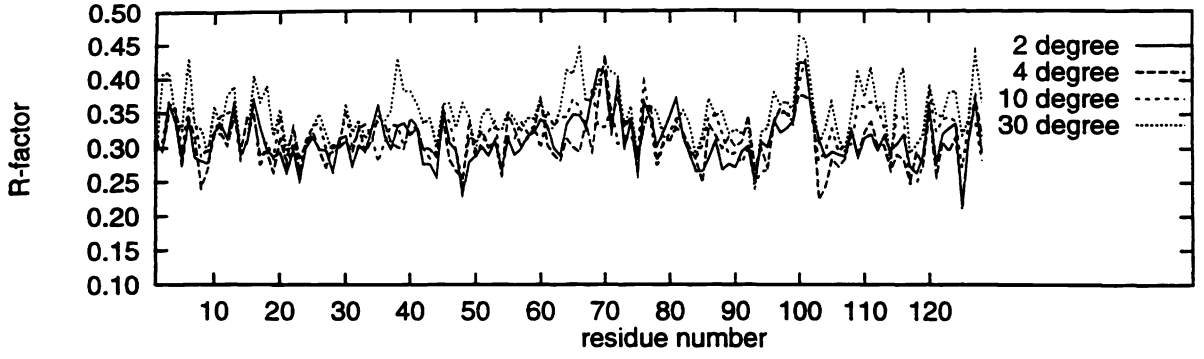

Figure 7: The Real-Space R-factors are shown on a per-residue basis, for the 2°, 4°, 10° and 30° angular interval Laue data

4 MONOCHROMATIC LOT DATA IN PROTEIN CRYSTALLOGRAPHY

4.1 Lysozyme LOT crystal test data

LOT patterns (e.g. figure 9a) were collected at SRS Daresbury station 9.5,[16] the SRS operated at 2.0 GeV and 274.5 mA with a 5 T Wiggler. An X-ray beam of wavelength 0.92Å with a horizontal beam divergence of 1 mrad and 0.3 mrad in the vertical, and a 0.2 mm collimator was used. The crystal-to-detector distance 232 mm was chosen to give a resolution of 2.5Å at the outer edges of the detector. Data were collected on a 90 mm radius MAR Image Plate(1200 x 1200 pixels and 0.15 mm pixel size). Two data sets were collected, each covering 68° oscillation range in total. The first data set (LOT-1) contains 1 image of 39° and 1 image of 29° . The second data set (LOT-2) contains 6 images of 10° and 1 image of 8°. The exposure time was 1 min/°. The images for the two LOT data sets were processed using MOSFLM,[52] scaled using SCALA and merged using AGROVATA both from the CCP4[38] program suite. LOT-2 data (truncated at 4Å) were combined with Laue data (2Å) using the SCALA program, and then merged into unique data set using AGROVATA. The final R-factors and completeness are summarised in Table 1.

data sets	R_{merge} (I)	*completeness*		
		∞ to $2d_{min}$	$2d_{min}$ to d_{min}	∞ to d_{min}
LOT-1	9.2%	88.6%	73.2%	75.4%
LOT-2	10.5%	87.5%	94.7%	93.7%
Laue	8.8%	50.5%	77.9%	74.1%
Combined	11.4%	94.0%	77.9%	80.1%

Table 1: R_{merge} and completeness for the four data sets discussed in section 4. Note the d_{min}'s are 2.5Å for LOT-1 and LOT-2, 2.0Å for Laue and Combined (ie.LOT-2 truncated to 4Å + Laue to 2Å)

The structure refinement of lysozyme was carried out using four data sets, ie LOT-1, LOT-2, Laue data set (singles and deconvoluted multiples) at 2.0Å (Laue), and LOT-2(to 4Å) combined with Laue (to 2.0Å) (Combined). The starting models used for LOT-2, Laue and Combined were from the PDB (6LYZ),[36] whilst

Downloaded From: http://opticalengineering.spiedigitallibrary.org/ on 02/17/2016 Terms of Use: http://spiedigitallibrary.org/ss/TermsOfUse.aspx

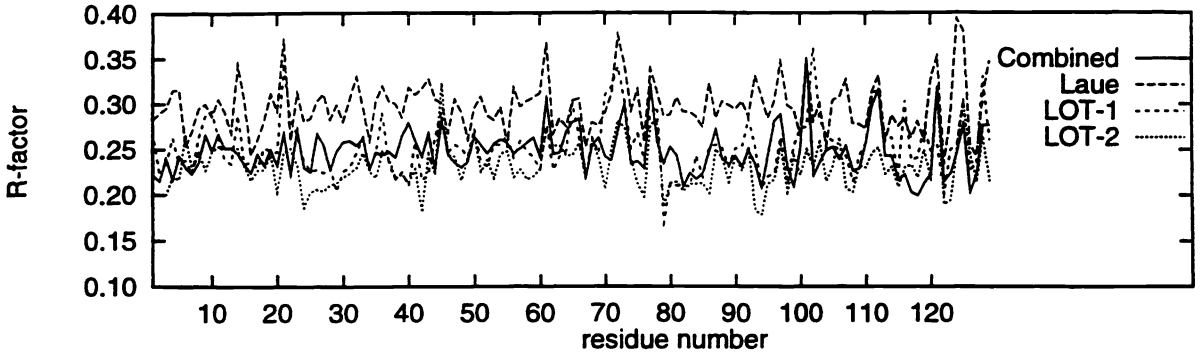

Figure 8: The Real-Space R-factors are shown on a per-residue basis, for the Combined set, the Laue set, LOT-1 and LOT-2

LOT-1 used the final protein model from LOT-2. The X-PLOR[37] program was used to refine the structure (40 cycles of positional refinement followed by 20 cycles of temperature refinement for each run). The O[40] program was used to examine the 2Fo-Fc and Fo-Fc maps after each run of XPLOR. PEAKMAX and WATERPEAK(CCP4[38] programs) were used to find possible water positions with peaks greater than 3σ in the Fo-Fc maps and good hydrogen-bond contacts. Some residues were adjusted to fit the 2Fo-Fc maps using O.[40] Figures 9b, 9c and 9d, show residue Phe 38 for the three data sets.

4.2 Structure refinement results

The crystallographic R-factors and R.M.S deviations of bond lengths, bond angles and torsional angles from ideality are summarised in Table 2. The Real-Space R-factors[40,53,54] (RSR) are also calculated which give direct

data sets	*R-factors*	*R.M.S deviations*		
	(F)	bond lengths	bond angles	torsional angles
LOT-1	17.6%	0.011Å	2.040°	22.803°
LOT-2	17.0%	0.010Å	1.916°	22.826°
Laue	19.9%	0.011Å	2.181°	22.762°
Combined	21.0%	0.010Å	2.016°	22.475°

Table 2: Refinement R-factors and r.m.s deviations for the four data sets discussed in section 4

insights into the quality of fitting between protein models and the electron density maps on a per-residue basis. They are shown in figure 8 for the four data sets. The average RSR factors for LOT-1, LOT-2, Laue and Combined are 25.2%, 23.1%, 29.8% and 24.7% respectively.

4.3 LOT development

With the good quality of data from LOT patterns to date, we are now exploring the use of 360° rotations onto a single image. For a full rotation of a crystal, each reciprocal lattice point will cross the Ewald sphere twice,

Downloaded From: http://opticalengineering.spiedigitallibrary.org/ on 02/17/2016 Terms of Use: http://spiedigitallibrary.org/ss/TermsOfUse.aspx

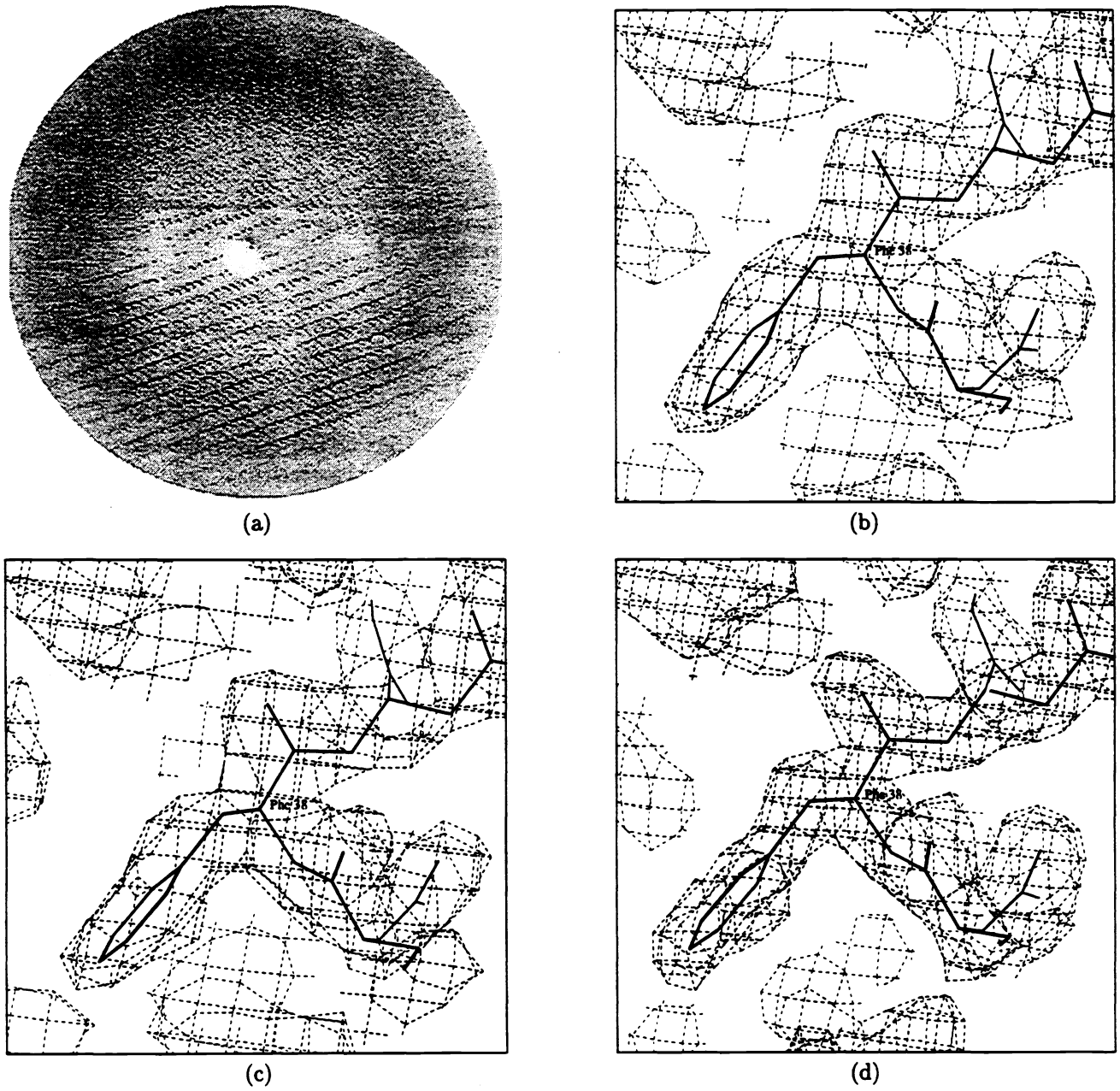

Figure 9: Tetragonal lysozyme LOT data results (a) LOT-1 diffraction image recorded on station 9.5 (39° range), (b) 2Fo-Fc electron density from LOT-1 data for Phe 38 at 2.5Å, (c) 2Fo-Fc electron density from LOT-2 data for Phe 38 at 2.5Å, (d) 2Fo-Fc electron density from combined (ie. LOT-2 truncated at 4Å and Laue data to 2Å). For details see section 4.

Downloaded From: http://opticalengineering.spiedigitallibrary.org/ on 02/17/2016 Terms of Use: http://spiedigitallibrary.org/ss/TermsOfUse.aspx

therefore, forming two distinct spots on the 2-D detector. We define here four categories of spots possibly existing in a LOT pattern. The percentage of each category depends on the resolution limit, crystal symmetry, crystal orientation and oscillation range. We define these spots as 'single spots', 'coincident symmetric spots', 'clustering symmetric spots' and 'overlap spots'. Single spots are spots from a single reflection. Coincident symmetric spots involve symmetry-related reflections(eg. (5,0,6), (-5,0,6), (0,5,6), (0,-5,6) which form a symmetric spot with multiplicity equal to 4 in a tetragonal space group with the crystal perfectly aligned and c* axis along the rotation axis) situated exactly at the same position(ie. exact overlaps) but without overlap with any other (h k l) group. When the crystal is mis-set, some coincident symmetric spots may split into single spots, coincident symmetric spots with lower multiplicities or 'clustering symmetric spots'. Some coincident symmetric spots or single spots may overlap with other (h,k,l) groups forming 'overlap spots'. The coincident symmetric spots can be integrated as single spots and the real intensity of each member is the total integrated intensity divided by their multiplicities. The clustering symmetric spots and overlap spots will be difficult to be deconvoluted into individual parts and may, in the early stages at least, be ignored.

Simulations of 360° LOT patterns using lysozyme($P4_32_12$) as a test sample have been carried out at 5.0Å resolution with the crystal perfectly aligned, misset along one axis, and misset along two axes. The statistics of numbers of spots and percentage completeness are summarised in Table 3. The very high completeness of data

missetting angles along a,b**	*total reflections*	*single reflections*		*coincident symmetric reflections*		*spatial overlap reflections*		*clustering symmetric reflections*		*unique reflections*	*completeness*
0°,0°	15888	0	0%	6520	41%	9368	59%	0	0%	260	41.7%
0°,6°	15892	372	2%	13500	85%	2020	13%	0	0%	620	99.5%
1°,6°	15896	9388	59%	164	1%	4932	31%	1412	9%	590	94.7%

Table 3: Statistics of 360° protein crystal (tetragonal lysozyme) LOT patterns for different crystal missettings. Note. The simulations assume the detector type is a 15 cm radius MAR image plate, resolution limit of 5Å and spot size 0.7 mm × 0.7 mm.

suggests that 360° LOT data collection is a feasible way to fill in the low-resolution hole (∞ to d_{max})in the Laue data, and allows the whole data to be recorded in a single image with the highest redundancy possible and avoiding any time overheads of detector read-out time. Most importantly of all if one contemplates rotating a crystal at the angular speed of a rotor arm in an ultracentrifuge (as a guide to a practical limit eg. 60000 rpm), then 1 revolution would be covered in 1 millisecond. At such speeds no detailed sequence of synchronization of shutters opening or closing is wanted and hence the recording of a full 360° of data onto one image is therefore being explored as a possible rapid diffraction data acquisition method.

5 SUMMARY: X-RAYS, ELECTRONS AND NEUTRONS

The opening up of the dimension of structural changes as a function of time or environmental conditions (temperature, pressure) is of considerable interest.[4,29] Since structure is related to function, insights into life or materials *processes* can be obtained. Critically the direct experimental monitoring of the perturbation of structures is needed to provide the basis to tether computer graphics simulations. In crystallography[1,3,4] over fibre diffraction[2] the huge challenge is to survey 3-D spatial rather than 2-D spatial X-ray data respectively in time. This has presented challenges in data collection strategies (Laue and monochromatic) as well as sources, optics and detector developments, and choice of suitable structural systems.[4,55]

In comparing X-rays and electrons, obviously the electron cross section of interaction is much larger and so very thin samples can be studied (e.g. proteins in membranes); this has the advantage that 'direct' freeze

Downloaded From: http://opticalengineering.spiedigitallibrary.org/ on 02/17/2016 Terms of Use: http://spiedigitallibrary.org/ss/TermsOfUse.aspx

trapping of altered structures on the millisecond time scale is feasible.[56,57] For 3-D samples such as crystals the time needed to freeze such a sample is exacerbated but of course it is 3-D crystals that provide the greatest structural detail. Cryo-crystallography is an option where processes are slowed down[58] but opens up questions of direct relevance of such structures to the in vivo state.[59] The continued development of rapid data collection for X-ray crystallography is therefore important.

The weakness of X-rays is in locating protons (H atoms) and yet this is a large area of enzymology. Neutrons lend themselves to finding protons. White beam synchrotron X-ray techniques[11] are finding adaptation at thermal neutron sources for quicker neutron data collection.[60]

6 ACKNOWLEDGEMENTS

We are grateful to the staffs of the synchrotron radiation sources at Daresbury SRS, Brookhaven NSLS and Grenoble ESRF for the provision of beam. SRS Station 9.5 has been funded in large part by the Swedish Research Council (NFR) as well as the UK SERC (now EPSRC) and the UK MRC to whom we are extremely grateful. The ESRF is a collaborative project involving twelve European partners. The EC Science Stimulation Plan and the SERC (now EPSRC) are thanked for grant support to JRH and NMA. EPSRC provides research studentships for GB, AD, and EHS. The family of Yeu Perng Nieh are thanked for his support. ST is funded by a Università di Trieste scholarship. Dr. J. Raftery is also thanked for computational support. The continuing support and interest of EEV in CCD developments is of immense benefit to this continuing work.

7 REFERENCES

1 J. R. Helliwell. *Macromolecular Crystallography with Synchrotron Radiation*, Cambridge University Press, UK, 1992.

2 G. Rosenbaum, K. C. Holmes and J. Witz. "Synchrotron radiation as a source for X-ray diffraction," *Nature*, 230:434, 1971.

3 J. R. Helliwell. "Optimisation of anomalous scattering and structural studies of proteins using synchrotron radiation," in *Proceedings of the Daresbury Study Weekend*, number DL/SCI/R13, pp. 1–6, 1979.

4 D. W. J. Cruickshank, J. R. Helliwell and L. N. Johnson, editors. *Time-resolved macromolecular crystallography*, The Royal Society and Oxford University Press, 1992.

5 J. R. Helliwell. "Synchrotron X-ray Crystallography Techniques: Time-Resolved Aspects of Data Collection," *Phil. Trans. R. Soc. Lond.*, (340):221–232, 1992.

6 K. Moffat, D. M. Szebenyi and D. Bilderback. "X-ray Laue Diffraction from Protein Crystals," *Science*, 223:1423–1425, 1984.

7 S. Weisgerber and J. R. Helliwell. "High-resolution Crystallographic Studies of Native Concanavalin A using Rapid Laue Data Collection Methods and the Introduction of a Monochromatic Large-angle Oscillation Technique (LOT)," *J. Chem. Soc. Faraday Trans.*, 89(15):2667–2675, 1993.

8 N. Sakabe, S. Ikemizu, K. Sakabe, T. Higashi, A. Nakagawa and N. Watanabe. "Weissenberg camera for macromolecules with imaging plate data-collection system at the Photon Factory - Present status and future plan," *Rev. Sci. Instrum.*, 66(2):1276–1281, 1995.

9 I. A. Andersson, I. J. Clifton, V. Fulop and J. Hajdu. *High speed high resolution data collection on spinach Rubisco using a Weissenberg camera at the Photon Factory*, in Crystallographic Computing V. Edited by D. Moras *et al.*. Oxford University Press, 1991.

Downloaded From: http://opticalengineering.spiedigitallibrary.org/ on 02/17/2016 Terms of Use: http://spiedigitallibrary.org/ss/TermsOfUse.aspx

10 W. L. Bragg. *The Development of X-ray Analysis*, p. 137, Bell and Sons, 1975.

11 D. W. J. Cruickshank, J. R. Helliwell and K. Moffat. "Multiplicity Distribution of Reflections in Laue Diffraction," *Acta Cryst.*, (43):656–674, 1987.

12 J. R. Helliwell. "Protein crystallography with synchrotron radiation," *J. Molec. Struct.*, (130):63–91, 1985.

13 J. R. Helliwell, J. Habash, D. W. J. Cruickshank, M. M. Harding, T. Greenhough, J. W. Campbell, I. J. Clifton, M. Elder, P. A. Machin, M. Z. Papiz and S. Zurek. "The Recording and Analysis of Synchrotron X-radiation Laue Diffraction Photographs," *J. Appl. Cryst.*, 22:483–497, 1989.

14 M. Lindahl, A. Liljas, J. Habash, S. Harrop and J. R. Helliwell. "The Sensitivity of the Synchrotron Laue Method to Small Structural Changes: Binding Studies of Human Carbonic Anhydrase II (HCAII)," *Acta Cryst.*, B(48):281–285, 1992.

15 A. D. Cameron, S. J. Smerdon, A. J. Wilkinson, J. Habash, J. R. Helliwell, T. Li and J. S. Olson. "Distal Pocket Polarity in Ligand Binding to Myoglobin: Deoxy and Carbonmonoxy Forms of a Threonine^{68}(E11) Mutant Investigated by X-ray Crystallography and Infrared Spectroscopy," *Biochemistry*, 32:13061–13070, 1993.

16 R. C. Brammer, J. R. Helliwell, W. Lamb, A. Liljas, P. R. Moore, A. W. Thompson and K. Rathbone. "A new protein crystallography station on the SRS wiggler beamline for very rapid Laue and rapidly tunable monochromatic experiments .1. Design principles, ray tracing and heat calculations," *Nucl. Instrum. Methods A*, 271(3):678–687, 1988.

17 N. M. Allinson, P. D. Carr, M. Colapietro, M. M. Harding, J. R. Helliwell, A. W. Thompson and S. Weisgerber. "Time-Resolved Synchrotron Laue Diffraction and its Application in Structural Molecular Biology and Materials Science," *Phase Transitions*, 39:145–160, 1992.

18 A. Deacon, J. Habash, S. J. Harrop, J. R. Helliwell, W. N. Hunter, G. A. Leonard, M. Peterson, A. Hadener, A. J. Kalb (Gilboa), N. M. Allinson, C. Castelli, K. Moon, S. McSweeney, A. Gonzalez, A. W. Thompson, S. Ealick, D. M. Szebenyi and R. M. Walter. "SR Instrumentation for optimized anomalous scattering and high resolution structure studies of proteins and nucleic acids," *Rev. Sci. Instrum.*, 2(66):1287–1292, 1995.

19 J. R. Helliwell, T. J. Greenhough, P. D. Carr, S. A. Rule, P. R. Moore, A. W. Thompson and J. S. Worgan. "Central data-collection facility for protein crystallography, small-angle diffraction and scattering at the Daresbury-laboratory synchrotron rariation source (SRS), England," *Journal of Physics E-Scientific Instruments*, 15(12):1363–1372, 1982.

20 J. R. Helliwell, M. Z. Papiz, I. D. Glover, A. W. Habash, J. Thompson, P. R. Moore, N. Harris, D. Croft and E. Pantos. "The Wiggler Protein Crystallography Workstation at the Daresbury SRS. Progress and Results," *Nucl. Instr. and Meth.*, (246):617–623, 1986.

21 P. F. Lindley, E. M. H. Duke and C. Nave *et al.*to be published.

22 Y. P. Nieh and J. R. Helliwell. "Time differences between Friedel reflections: Accuracy of crystal setting and requirements on beam stability," *J. Synchrotron Rad.*, 2:79–82, 1995.

23 I. J. Clifton, M. Elder and J. Hajdu. "Experimental Strategies in Laue Crystallography," *J. Appl. Cryst.*, 24:267–277, 1991.

24 J. R. Helliwell. "Macromolecular crystallography beamline," in *ESRF Red Book*, pp. 329–340, 1987.

25 M. Wulff ESRF Newsletter, 1994.

26 J. P. Moy and S. Gibney. "Low Energy X-ray Image Intensifier Development Phase 1 Report," Preliminary Report EXP/JGM/SG/92/91, ESRF, Grenoble, France, December 1992.

Downloaded From: http://opticalengineering.spiedigitallibrary.org/ on 02/17/2016 Terms of Use: http://spiedigitallibrary.org/ss/TermsOfUse.aspx

27 N. M. Allinson, R. Brammer, J. R. Helliwell, S. Harrop, B. G. Magorrian and T. Wan. "Charge coupled device (CCD) area detector for on-line (40-80 ms) acqusition of Laue diffraction data from protein crystals," *J. X-ray Sci. Technol.*, 1(143), 1989.

28 N. M. Allinson, M. Colapietro, J. R. Helliwell, K. J. Moon, A. W. Thompson and S. Weisgerber. "Charge-Coupled Imagers for Time-Resolved Macromolecular Crystallography," *Rev. Sci. Instrum.*, 63(1):664–666, Jan 1992.

29 P. Coppens. *Synchrotron Radiation in Crystallography*, Academic Press, 1992.

30 K. Moon, N. M. Allinson and J. R. Helliwell. "High-Speed CCD Aquisition System," *Nucl. Instr. and Meth.*, A(348):631–634, 1994.

31 J. Hajdu, S. C. Almo, G. K. Farber, J. K. Prater, G. A. Petsko, S. Wakatsuki, I. J. Clifton and V. Fülöp. Edited by D. Moras *et al.*. "On the Limitations of the Laue Method when Applied to Crystals of Macromolecules," Crystallographic Computing V, pp. 29–49. OUP, 1991.

32 Z. Ren and K. Moffat. "Laue crystallography for analysing rapid reactions," *J. Synchrotron Rad.*, (1):18–82, 1994.

33 A. Cassetta, A. Deacon, C. Emmerich, J. Habash, J. R. Helliwell, S. McSweeney, E. Snell, A. W. Thompson and S. Weisgerber. "The Emergence of the Synchrotron Laue Method for Rapid Data Collection from Protein Crystals," *Proc. R. Soc. Lond.*, A(442):177–192, 1993.

34 A. Deacon, J. Habash, A. W. Thompson, J. R. Helliwell, S. McSweeney and E. H. Snell. "The development of a transmission mirror to control λ_{max} in Laue diffraction," *J. Synchrotron Rad.*, 1995, To be submitted.

35 J. W. Campbell and Q. Hao. "Evaluation of Reflection Intensities for the Components of Multiple Laue Diffraction Spots. II. Using the Wavelength Normalisation Curve," *Acta Cryst.*, A(49):889–893, 1993.

36 R. Diamond. "Real space refinement of the structure of hen egg-white lysozyme," *J. Mol. Biol.*, (82):371–391, 1974.

37 A. T. Brünger. *X-PLOR Version 3.1 A System for X-ray Crystallography and NMR*, Yale University Press, New Haven and London, 1992.

38 Collaborative Computational Project Number 4. "The CCP4 Suite: Programs for Protein Crystallography," *Acta Cryst.*, D(50):760–763, 1994.

39 T. A. Jones and L. Liljas. "Crystallographic refinement of macromolecules having non-crystallographic symmetry," *Acta Cryst.*, (40):50–57, 1984.

40 T. A. Jones, J. Y. Zou, S. W. Cowan and M. Kjelgaard. "Improved methods for building protein models in electron density maps and the location of errors in these models," *Acta Cryst.*, A(47):110–119, 1991.

41 C. Ramakrishnan and G. N. Ramachandran. "Stereochemical criteria for polypeptide and protein chain conformation," *Biophys. J.*, (5):909–933, 1965.

42 J. W. Campbell, A. Deacon, J. Habash, J. R. Helliwell, S. McSweeney, H. Quan, J. Raftery and E. Snell. "Electron Density Maps of Lysozyme Calculated using Synchrotron Laue Data Comprising Singles and Deconvoluted Multiples," *Bull. Mater. Sci.*, 17(1):1–18, 1994.

43 T. L. Blundell and L. N. Johnson. *Protein Crystallography*, Academic Press, 1976.

44 P. J. Artymiuk, C. C. F. Blake, D. W. Rice and K. S. Wilson. "The structures of the monoclinic and orthorhombic forms of hen egg-white lysozyme at 6Å resolution," *Acta Cryst.*, B(38):778–783, 1982.

45 J. W. Campbell. "LAUEGEN, an X-windows-based program for the processing of Laue X-ray diffraction data," *J. Appl. Cryst.*, 28:228–236, 1995.

Downloaded From: http://opticalengineering.spiedigitallibrary.org/ on 02/17/2016 Terms of Use: http://spiedigitallibrary.org/ss/TermsOfUse.aspx

46 P. D. M. Fitzgerald. "MERLOT, an integrated package of computer programs for the determination of crystal structures by molecular replacement," *Acta Cryst.*, (21):273–278, 1988.

47 J. H. Naismith, J. Habash, S. Harrop, J. R. Helliwell, W. N. Hunter, T. C. M. Wan and S. Weisgerber. "Refined structure of Cadmium-Substituted concanavalin A at 2.0Å resolution," *Acta Cryst.*, (50):561–571, 1993.

48 R. A. Laskowski, M. W. MacArthur, D. S. Moss and J. Thornton. "PROCHECK - A program to check the stereochemical quality of protein structures," *J. Appl. Cryst.*, 26(2):283–291, 1993.

49 S. Weisgerber and J. R. Helliwell. "Chicken Egg-White Lysozyme Crystals Grown in Microgravity and on Earth for a Comparison of their Respective Perfection," *Joint CCP4 and ESF-EACBM Newsletter on Protein Crystallography*, (29):10–13, 1993.

50 J. R. Helliwell, E. H. Snell and S. Weisgerber. "An Investigation of the Perfection of Lysozyme Protein Crystals Grown in Microgravity (Spacehab-1 and IML-2) and on Earth," in *Proceedings of the Berlin Microgravity Meeting.*. Springer Verlag, 1995, in press.

51 C. C. F. Blake, G. A. Mair, A. C. T. North, D. C. Philips and V. R. Sarma *Proc. Roy. Soc. (London)*, B(167):365, 1967.

52 A. J. Wonacott, S. Dockerill and P. Brick MOSFLM program. Unpublished notes.

53 R. Diamond. "A Real-Space Refinement Procedure for Proteins," *Acta Cryst.*, A(27):436–452, 1971.

54 R. K. Wierenga, K. H. Kalk and W. G. J. Hol. "Structure determination of the glycosomal triosephosphate isomerase from trypanosoma-brucei-brucei at 2.4Å resolution," *J. Mol. Biol.*, (1):109–121, 1987.

55 E. F. Pai. "Time-resolved macromolecular crystallography," *Current Opinion in Structural Biology*, (2):821–827, 1992.

56 S. Subramaniam, M. Gerstein, D. Desterfelt and R. Henderson. "Electron diffraction analysis of structural changes in the photocycle of bacteriororhodopsin," *EMBO J.*, 12:1–8, 1993.

57 J. Berriman and N. Unwin. "Analysis of transient structure by cryo-microscopy combined with rapid measuring of spray droplets," *Ultramicroscopy*, 1995, In press.

58 T. Y. Teng, V. Srajer and K. Moffat. "Photolysis-induced structural-changes in single-cyystals of carbonmonoxy myoglobin at 40 K," *Nature Structural Biology*, 1(10):701–705, 1994.

59 B. F. Rasmussen, A. M. Stock, D. Ringe and G. A. Petsko. "Crystalline ribonuclease-A loses function below the dynamic transition at 220-K," *Nature*, 357(6377):423–424, 1992.

60 C. Wilkinson and M. S. Lehmann. "Quasi-Laue neutron diffractometer," *Nucl. Inst. Methods*, 310(1-2):411–415, 1991.

Downloaded From: http://opticalengineering.spiedigitallibrary.org/ on 02/17/2016 Terms of Use: http://spiedigitallibrary.org/ss/TermsOfUse.aspx